

Anomalous Dispersion Behavior of Multiple-Wave X-Ray Diffraction at Absorption Edges: Determination of Phase Change at Resonance

Yuri P. Stetsko,^{1,3} Gong-Yih Lin,¹ Yi-Shan Huang,¹ Chun-Hsiung Chao,¹ and Shih-Lin Chang^{1,2}

¹Department of Physics, National Tsing Hua University, Hsinchu, Taiwan, Republic of China 300

²Synchrotron Radiation Research Center, Hsinchu, Taiwan, Republic of China 300

³Chernovtsy State University, Chernovtsy 274012, Ukraine

(Received 7 August 2000)

The effects of anomalous dispersion (resonance) on multiple reflection of x rays and their interference in crystals at atomic absorption edges are studied. Intensity ratios of two inversion-symmetry-related multiple diffractions at or near absorption edges exhibit highly phase-sensitive profiles with strong asymmetric characteristics, unlike those far from the edges. A new resonance perturbation Bethe approach is developed to explain this behavior. This leads to direct determination of the phase change for x-ray reflections at resonance.

DOI: 10.1103/PhysRevLett.86.2026

PACS numbers: 61.10.Eq, 61.10.Kw

Use of x-ray scattering/diffraction for atoms in excited states or under resonance conditions is currently an important experimental trend of probing atomic and electronic structures of matter. Based on this, several techniques have been developed, including diffraction anomalous fine structure [1], x-ray resonance diffraction [2], multiwavelength anomalous dispersion for macromolecular crystals [3], etc. [4]. All of these involve simple Bragg diffraction, the so-called two-wave diffraction. Recently, the method of using multiple-wave diffraction, far from an excited situation (absorption edges), has been found useful in studying phase transformations in crystals [5], interaction of electric fields with crystals [6,7], and plasma diagnosis [8]. More importantly, multiple diffraction is capable of solving the phase problem [9–14], a long-standing topic in diffraction physics and crystallography [15].

From a physics point of view, it would be interesting to study multiple-wave diffraction from a crystal under excitation conditions, for example, at an absorption edge of a constituent atom. Then, several fundamental questions can be asked to understand the interaction of an x-ray wave field with atoms in electronic transitions. For example, how is the diffraction intensity related to the anomalous dispersion caused by the resonance between x-ray waves and the atoms? What additional information can be extracted from multiple-wave interaction at resonance? Attempts to clarify these issues had been pursued experimentally and numerically [16] but without success, mainly, because the photon energies used are far (around 500–800 eV) from that of absorption edges ($\Delta E \sim 20$ eV). A similar investigation in the same energy region has also been reported in Ref. [13]. In this Letter, we present a rather complete and detailed experimental investigation using two inversion-symmetry-related (ISR) three-wave diffractions at absorption edges. A resonance perturbation Bethe (RPB) approach is newly developed to account for the observed anomalous behavior and to provide fundamental understanding of x-ray multiple-wave interaction at resonance. Extra information, such as

the spectral distribution of reflection phase change due to x-ray resonance, is determined.

Multiple-wave diffraction of x rays in crystals takes place when several sets of atomic planes simultaneously satisfy Bragg's law. In a three-wave (O, G, L) diffraction, the crystal is aligned for the primary G reflection and then rotated (the azimuthal ψ scan) around the reciprocal lattice vector of the G reflection to satisfy Bragg's law for the secondary L reflection. The interaction among the G reflection and the detoured reflection, which is produced by the L reflection via the $G - L$ coupling, modifies the intensity of the primary reflection. This intensity modification can be explained by employing the perturbational Bethe [10,11] and the Born [12,17] or expanded distorted-wave Born [18] approximations. Generally, the intensity modification is related to the phases δ_G , δ_L , and δ_{G-L} of G , L , and $G - L$ reflections and also to the phases δ_{-G} , δ_{-L} , and δ_{L-G} of the inverse reflections $-G$, $-L$, and $L - G$. More precisely, it is related [10,11] to the triplet phases $\delta_+ = -\delta_G + \delta_L + \delta_{G-L}$ and $\delta_- = -\delta_{-G} + \delta_{-L} + \delta_{L-G}$ of the structure-factor triplets $F_L F_{G-L} / F_G$ and $F_{-L} F_{L-G} / F_{-G}$, and also to the phase sums, hereafter called resonance phases, $\Delta_G = \delta_G + \delta_{-G}$, $\Delta_L = \delta_L + \delta_{-L}$, and $\Delta_{G-L} = \delta_{G-L} + \delta_{L-G}$ of the structure-factor products $F_G F_{-G}$, $F_L F_{-L}$, and $F_{G-L} F_{L-G}$, respectively. Far from the absorption edges, for negligibly small anomalous dispersion, the values of Δ_G , Δ_L , Δ_{G-L} , and triplet resonance phase $\Delta = \delta_+ + \delta_- \equiv -\Delta_G + \Delta_L + \Delta_{G-L}$ are close to zero. In this case, the Friedel pairs of ψ scanned profiles, for two ISR three-wave reflections (O, G, L) and ($O, -G, -L$), can be described by quasiuniversal functions [19] with the same asymmetry. At the absorption edges, where Friedel's law is no longer valid, the values of all resonance phases can differ from zero dramatically that show anomalous behavior of x-ray multiple-wave diffraction. These are reported in this Letter. The resonance phases are therefore the actual phase changes due to resonance.

The behavior of three-wave diffraction is investigated for a noncentrosymmetric crystal GaAs at the K -absorption edges of gallium ($E_{k(\text{Ga})} = 10369$ eV) and arsenic ($E_{k(\text{As})} = 11869$ eV). The symmetrical Bragg reflection 222 with a π -polarized incident radiation is employed as the reflection G . The experiments were carried out at the wiggler beam line SB-05 of the Synchrotron Radiation Research Center. The vertical and horizontal angular divergences and the energy spread of the beam were 0.010° , 0.025° , and 2 eV, respectively. The beam energy could be stepped 0.2 eV by turning the double-crystal Si(111) monochromator.

Figures 1 and 2 show the ψ scanned three-wave profiles at the Ga and As K edges for two ISR cases “+” (000, 222, $3\bar{3}\bar{1}$) and “-” (000, $\bar{2}\bar{2}\bar{2}$, $\bar{3}\bar{3}\bar{1}$). The direction of the ψ scanning corresponds to the movement of the reciprocal lattice points of the reflections $3\bar{3}\bar{1}$ and $\bar{3}\bar{3}\bar{1}$ towards the Ewald sphere. Figures 1 and 2 show high sensitivity of the profile shape to the incident photon energy. The changing of the profile asymmetry is observed for both ISR cases when the energy is crossing the As K edge (Fig. 2), while only for the case “-” when crossing the Ga K edge (Fig. 1).

The RPB approach with the improved resonance term for the secondary reflection is developed to account for the observed behavior. According to the perturbational approach, the three-wave wave field $\vec{D}_{G(3)}$ is the sum of the two-wave $\vec{D}_{G(2)}$ and the detoured $\vec{D}_{G(d)}$ wave fields,

$$\vec{D}_{G(3)} = \vec{D}_{G(2)} + \vec{D}_{G(d)} = -\chi_G \vec{P}_{GL} D_O / A_G, \quad (1)$$

where D_O is the magnitude of the incident wave field, and

$$\vec{P}_{GL} = \vec{p}_{G(2)} + f_+ e^{i\delta_+} \vec{p}_{G(d)} / A_L \quad (2)$$

is the perturbational polarization vector; $\vec{p}_{G(2)} = \vec{s}_G \times (\vec{s}_G \times \vec{p})$ and $\vec{p}_{G(d)} = \vec{s}_G \times \{\vec{s}_G \times [\vec{s}_L \times (\vec{s}_L \times \vec{p})]\}$ are the polarization vectors of the primary and detoured

diffracted waves; \vec{p} ($= \vec{\sigma}$ or $\vec{\pi}$) is the polarization state of incident wave; \vec{s}_G and \vec{s}_L are the unit vectors of the primary and secondary diffracted waves; $A_H = -k^2/K_H^2 + (1 - \chi_O)$ for $H = G, L$ is the resonance term; and χ_H is the Fourier component of the crystal polarizability proportional to the structure factors F_H ($H = G, L, G - L$). The factor f_+ is defined as $f_+ = |\chi_{G-L}| |\chi_L| / |\chi_G|$.

According to the Bethe approximation [10,11], the resonance term A_G is related to the solution of the perturbed dispersion equation. For a symmetrical Bragg primary reflection, it is expressed [11] as

$$A_G = -z_G + \sqrt{z_G^2 - \chi_G \chi_{-G} P_{GL}^p P_{-(GL)}^p}, \quad (3)$$

where $P_{GL}^p = (\vec{P}_{GL} \cdot \vec{p})$ and $P_{-(GL)}^p = (\vec{P}_{-(GL)} \cdot \vec{p})$. Here, $\vec{P}_{-(GL)}$ is the same as \vec{P}_{GL} except for changing all the reflections H to $-H$. z_G is a function of the deviation $\Delta\theta_G$ from Bragg angle θ_G :

$$z_G = \Delta\theta_G \sin 2\theta_G + \chi_O + (a_O \chi_L \chi_{-L} + a_G \chi_G \chi_{-L} \chi_{L-G}) / 2A_L, \quad (4)$$

where $a_O = a_G = 1 - (\vec{s}_L \cdot \vec{\sigma})^2$ for a σ polarized and $a_O = 1 - (\vec{s}_L \cdot \vec{\pi}_O)^2$, $a_G = 1 - (\vec{s}_L \cdot \vec{\pi}_G)^2$ for a π -polarized incident waves.

For the resonance term A_L , the two-wave approximation is employed. For a given nonsymmetrical Bragg two-wave reflection L , the A_L is a function of $\Delta\theta_G$ and azimuthal angle $\Delta\psi_G$ of the primary reflection:

$$A_L = -z_L + \sqrt{z_L^2 - a_O \chi_L \chi_{-L} \gamma_L / \gamma_G}, \quad (5)$$

where γ_G and γ_L are the direction cosines of \vec{s}_G and \vec{s}_L with respect to the inward surface normal, and

$$z_L = W_\psi \Delta\psi_G + W_\theta \Delta\theta_G + \chi_O (1 + \gamma_L / \gamma_G) / 2, \quad (6)$$

with $W_\theta = \sqrt{1 - (\vec{s}_L \cdot \vec{\sigma})^2 - \gamma_L^2} \sin \theta_G + \sin 2\theta_G \gamma_L / 2\gamma_G$ and $W_\psi = (\vec{s}_L \cdot \vec{\sigma}) \cos \theta_G$. In Eqs. (3) and (5) the square roots are taken with positive imaginary parts.

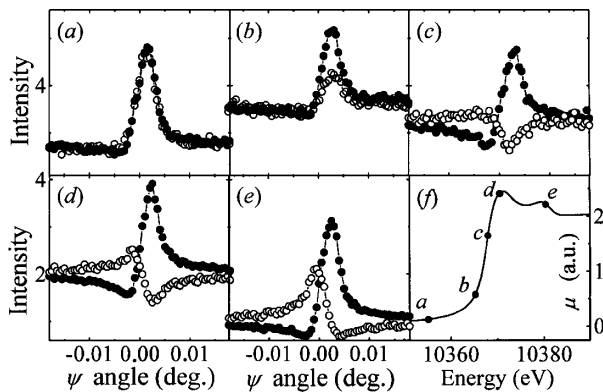


FIG. 1. The measured three-wave peak profiles at the Ga K edge. Profiles (a)–(e) are obtained for energies indicated in (f) on the absorption spectrum of GaAs at the edge. Intensities are given in units of two-wave intensity for the case (e). Solid circles: “+” case; open circles: “-” case.

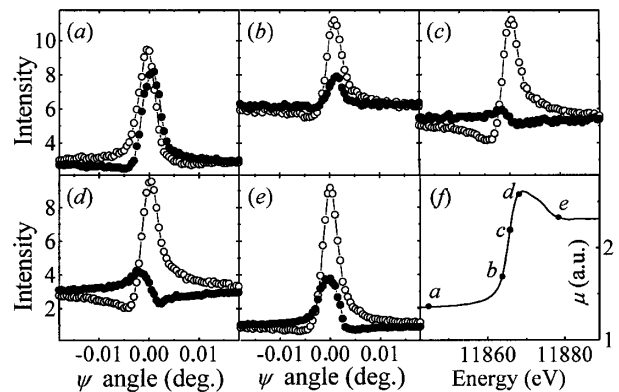


FIG. 2. The measured three-wave peak profiles at the As K edge. Profiles (a)–(e) are obtained for energies indicated in (f) on the absorption spectrum of GaAs at the edge. Intensities are given in units of two-wave intensity for the case (e). Solid circles: “+” case; open circles: “-” case.

Figure 3 shows the semi-integral profiles $R_G(\Delta\psi_G) = \int |\vec{D}_{G(3)} \vec{D}_{G(3)}^*| d(\Delta\theta_G)$ calculated for GaAs(000, 222, 33 $\bar{1}$) by the RPB approach. The atomic scattering factors due to anomalous dispersion [see Figs. 3(c) and 3(g)] are used for these calculations [20]. For comparison, the semi-integral profiles obtained by direct dynamical calculation [21] are also shown in Fig. 3. The excellent agreement between the results obtained by the two approaches is observed. Figure 3 shows qualitatively the same behavior for calculated profiles as that obtained experimentally. Clearly, the Born approximation, using a two-wave approach for A_G , cannot give such satisfactory agreement at the absorption edges.

Analysis for the function $R_G(\Delta\psi_G)$ is complicated. Therefore, to reveal the main anomalous behavior of the profiles, we use additional approximations. The dependence of z_L on the angle $\Delta\theta_G$ is neglected. In this case, $R_G(\Delta\psi_G) \approx |\vec{P}_{GL} \vec{P}_{GL}^*| I(\Delta\psi_G)$, where $I(\Delta\psi_G) = D_O^2 \int (1/|A_G A_G^*|) d(\Delta\theta_G)$. The term $|\vec{P}_{GL} \vec{P}_{GL}^*|$ depends

$$R(\Delta\psi_G) \approx |\chi_G/\chi_{-G}|^2 \{1 + (2\Delta\psi_G d_c - 2\eta_L d_s + d)/[(\Delta\psi_G - \psi_-)^2 + q_-^2]\}, \quad (7)$$

where the width $\eta_L = -\chi_O''(1 + \gamma_L/\gamma_G)/2 + \sqrt{a_O |\chi_L| |\chi_{-L}| \gamma_L/\gamma_G}$, $d_c = p_s(f_+ \cos\delta_+ - f_- \cos\delta_-)$, $d_s = p_s(f_+ \sin\delta_+ - f_- \sin\delta_-)$, $d = p_d(f_+^2 - f_-^2)$, $\psi_- = -p_s f_- \cos\delta_-$, $q_-^2 = (\eta_L - p_s f_- \cos\delta_-)^2 + f_-^2 (p_d - p_s^2)$, $p_s = (\vec{p}_{G(2)} \cdot \vec{p}_{G(d)})/p_{G(2)}^2$, $p_d = p_{G(d)}^2/p_{G(2)}^2$, and $f_- = |\chi_{L-G}| |\chi_{-L}|/|\chi_{-G}|$. From Eq. (7), it follows that d_c is roughly proportional to $\sin(\Delta/2) \sin(\Delta_d/2)$, where $\Delta_d = \delta_+ - \delta_-$ is the phase difference. For the clarifica-

tion of the behavior of peak profiles, Figs. 4(a) and 4(c) show the distributions of phases δ_+ , δ_- , $\Delta/2$, and $\Delta_d/2$ calculated with the dispersion corrections [20]. Consider the three spectral regions: region I— $E < E_{k(\text{Ga})}$; region II— $E_{k(\text{Ga})} < E < E_{k(\text{As})}$; region III— $E > E_{k(\text{As})}$. In region I, Δ and d_c are close to zero, and therefore the ratio $R(\Delta\psi_G)$ is practically a symmetrical function close to a Lorentzian, and the two ISR cases have the same asymmetry of peak profiles. This is the characteristic [19] of the peak profiles far from absorption edges. When the energy approaches the Ga K edge, the ratio becomes slightly asymmetrical [see Fig. 3(a)], and the asymmetry increases dramatically in region II with increasing Δ

According to [22], this ratio can be estimated as

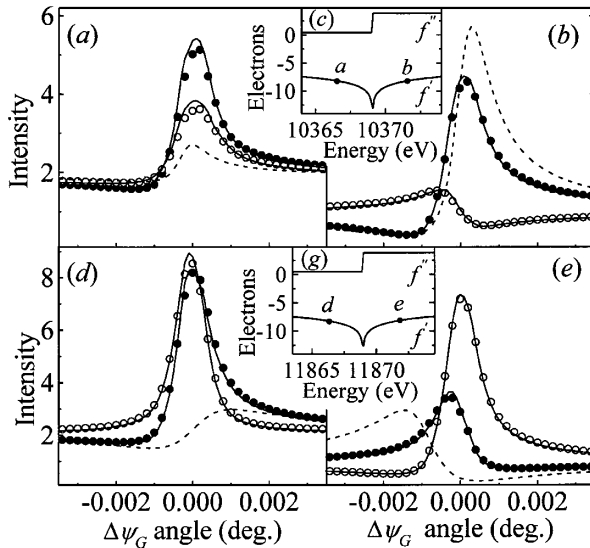


FIG. 3. The three-wave peak profiles at the (a)–(b) Ga K edge and (d)–(e) As K edge obtained by the RPB approach (solid lines) and by direct dynamical calculation (solid circles: “+” case; open circles: “–” case). Profiles are calculated for energies indicated in (c) and (g) of the dispersion corrections f' and f'' of the correspondent K edges. Intensities (a)–(b) and (d)–(e) are given in units of two-wave intensity for cases (b) and (e), respectively. The dash curves are the ratios $R(\Delta\psi_G)$ explained in the text.

tion of the behavior of peak profiles, Figs. 4(a) and 4(c) show the distributions of phases δ_+ , δ_- , $\Delta/2$, and $\Delta_d/2$ calculated with the dispersion corrections [20]. Consider the three spectral regions: region I— $E < E_{k(\text{Ga})}$; region II— $E_{k(\text{Ga})} < E < E_{k(\text{As})}$; region III— $E > E_{k(\text{As})}$. In region I, Δ and d_c are close to zero, and therefore the ratio $R(\Delta\psi_G)$ is practically a symmetrical function close to a Lorentzian, and the two ISR cases have the same asymmetry of peak profiles. This is the characteristic [19] of the peak profiles far from absorption edges. When the energy approaches the Ga K edge, the ratio becomes slightly asymmetrical [see Fig. 3(a)], and the asymmetry increases dramatically in region II with increasing Δ

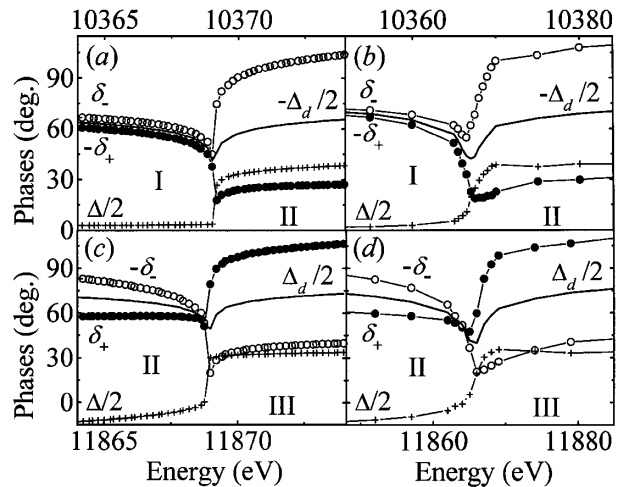


FIG. 4. The distributions of the phases δ_+ , δ_- , $\Delta/2$, and $\Delta_d/2$: the calculated ones for the (a) Ga K edge and (c) As K edge; the experimentally determined ones for the (b) Ga K edge and (d) As K edge.

[see Fig. 3(b)]. In regions II and III at the As K edge, the changing of the ratio asymmetry is observed [see Figs. 3(d) and 3(e)] that is accompanied with the changing of the sign of Δ [see Fig. 4(c)]. The change of the ratio asymmetry is independent of the change of asymmetry of the individual peak profiles. The latter occurs when the phases δ_+ or δ_- cross over the values around $\pm 90^\circ$. All the considered reflections give the comparably large contributions to the change of the triplet phases δ_+ and δ_- at the absorption edges. For the “weak” reflection $G(222)$ of the zinc blende structure, the change of the phase around 25° for the Ga K edge and 36° for the As K edge in the energy regions shown in Fig. 4 is mainly determined by the change of the imaginary part f'' [see Figs. 3(c) and 3(g)], while for the “strong” reflections $L(33\bar{1})$ and $G - L(\bar{1}\bar{1}3)$, the change of the phases (around 19° and 17° for L ; and 16° and 15° for $G - L$) is mainly related to the change of the real part f' .

Figures 4(b) and 4(d) show the distributions of phases δ_+ , δ_- , $\Delta/2$, and $\Delta_d/2$ determined from the best fit to the pairs of the experimental profiles for the two ISR cases with that obtained by the RPB approach using various values of the dispersion corrections f' and f'' . The use of the RPB approach to fit the pairs of the profiles obtained by the direct dynamical calculation gives the accuracy better than 2° for the phase determination, while the estimate of the directly calculated profiles from the methods (for example, [19,22]), conventionally used far from absorption edges, gives at the absorption edges an accuracy worse than 20° . Note that our aim is not to demonstrate the phase determination at absorption edges, because there is no practical necessity to go to the absorption edges for phase determination by the multiple-wave diffraction method, but to determine the spectral distribution of the resonance phase, namely, the reflection phase change due to resonance. Also, such highly sensitive behavior of the ratios could not be realized for every three-wave diffraction. It could be realized only for the case in which the phase Δ is changed dramatically with the changing of the incident photon energy. This takes place mainly when the direction of changing Δ_G is opposite to that of Δ_L and Δ_{G-L} .

In conclusion, the anomalous behavior of multiple-wave x-ray diffraction at the absorption edges is experimentally observed and theoretically fitted for the first time. The changing of the ratio asymmetry of the profiles for the two ISR cases results from the anomalous dispersion corrections in the structure factors due to the significant change of the resonance phase at the absorption edge. The RPB

approach is developed to account for this behavior. Excellent agreement between the experimental and theoretical results is obtained. The proposed experimental and theoretical approaches allow for the determination of the changes of x-ray reflection phases under resonance conditions with a high accuracy. This provides a highly sensitive way for experimental investigation of the spectral distribution of reflection phase change due to the resonance.

The authors are indebted to the Ministry of Education and the National Science Council for financial support under Contract No. 90-FA04-AA.

-
- [1] H. Stragier, J. O. Cross, J. J. Rehr, L. B. Sorensen, C. E. Bouldin, and J. C. Woicik, *Phys. Rev. Lett.* **69**, 3064 (1992).
 - [2] J. P. Attfield, *Nature (London)* **343**, 46 (1990).
 - [3] W. A. Hendrickson, *Science* **254**, 51 (1991).
 - [4] M. M. Woolfson and H. F. Fan, *Physical and Non-physical Methods of Solving Crystal Structures* (Cambridge University, Cambridge, England, 1995).
 - [5] S. L. Chang, *Appl. Phys. Lett.* **37**, 819 (1980).
 - [6] L. H. Avanci, L. P. Cardoso, S. E. Girdwood, D. Pugh, J. N. Sherwood, and K. J. Roberts, *Phys. Rev. Lett.* **81**, 5426 (1998).
 - [7] L. H. Avanci, L. P. Cardoso, J. M. Sasaki, S. E. Girdwood, K. J. Roberts, D. Pugh, and J. N. Sherwood, *Phys. Rev. B* **61**, 6507 (2000).
 - [8] B. S. Fraenkel, *Appl. Phys. Lett.* **36**, 341 (1980); **41**, 234 (1982).
 - [9] R. Colella, *Acta Crystallogr. Sect. A* **30**, 413 (1974).
 - [10] H. J. Juretschke, *Phys. Rev. Lett.* **48**, 1487 (1982); *Phys. Lett.* **92A**, 183 (1982).
 - [11] S. L. Chang, *Multiple Diffraction of X-Rays in Crystals* (Springer-Verlag, Heidelberg, 1984), Sects. 5.1 and 7.1.
 - [12] S. L. Chang, *Int. J. Mod. Phys. B* **6**, 2987 (1992).
 - [13] E. Weckert and K. Hümmer, *Acta Crystallogr. Sect. A* **53**, 108 (1997).
 - [14] S. L. Chang, Y. S. Huang, C. H. Chao, M. T. Tang, and Yu. P. Stetsko, *Phys. Rev. Lett.* **80**, 301 (1998).
 - [15] H. A. Hauptman, *Phys. Today* **42**, No. 11, 24 (1989).
 - [16] S. L. Chang, *Phys. Rev. B* **33**, 5848 (1986).
 - [17] Q. Shen, *Acta Crystallogr. Sect. A* **42**, 525 (1986).
 - [18] Q. Shen, *Phys. Rev. Lett.* **83**, 4784 (1999); *Phys. Rev. B* **61**, 8593 (2000).
 - [19] S. L. Chang, Yu. P. Stetsko, Y. S. Huang, C. H. Chao, F. J. Liang, and C. K. Chen, *Phys. Lett. A* **264**, 328 (1999).
 - [20] D. T. Cromer, *J. Appl. Crystallogr.* **16**, 437 (1983).
 - [21] Yu. P. Stetsko and S. L. Chang, *Acta Crystallogr. Sect. A* **53**, 28 (1997).
 - [22] S. L. Chang and M. T. Tang, *Acta Crystallogr. Sect. A* **44**, 1065 (1988).